

## Characterization of flame sprayed NiCrBSiMo coatings deposited with different spraying parameters

Haideé Ruiz-Luna<sup>a,✉</sup>, Karla O. Méndez-Medrano<sup>b</sup>,  
Miguel Montoya Dávila<sup>b</sup>, Víctor H. Baltazar-Hernández<sup>b</sup>

<sup>a</sup>CONACYT – Universidad Autónoma de Zacatecas, Unidad Académica de Ingeniería I,  
Av. Ramón López Velarde 801, 98000, Zacatecas, Zac., México

<sup>b</sup>Universidad Autónoma de Zacatecas, Unidad Académica de Ingeniería I,  
Av. Ramón López Velarde 801, 98000, Zacatecas, Zac., México

✉ Corresponding author: [hruizlu@conacyt.mx](mailto:hruizlu@conacyt.mx)

Submitted: 18 October 2019; Accepted: 10 February 2020; Available On-line: 28 August 2020

**ABSTRACT:** Optimization of processing parameters of a Ni-based coating is reported here. Three deposition variables were evaluated, *viz.* stand-off distance, flame chemistry, and nozzle diameter, on the crystal structure, porosity content, hardness and thickness of the coatings. The analysis was divided into two stages: firstly, the influence of the stand-off distance on the structural and microstructural characteristics of the coatings was determined. In the second stage, a simple 2<sup>2</sup> factorial design of experiments was employed to investigate the effect of the nozzle diameter and flame chemistry on the porosity, hardness and thickness of the coatings. Results indicated that porosity was strongly influenced by the stand-off distance. Flattening of the particles was achieved at intermediate distance decreasing the porosity; whereas the later increases for short or long distances as a result of the extended or limited particle deformation at impact, respectively. Regarding the nozzle diameter and flame chemistry, results revealed that the former has the predominant effect on the microstructure and hardness of the coatings. Small nozzle diameter and neutral flame reduce the porosity and increase the hardness of the coatings. NiCrBSiMo coatings with low porosity and high hardness using a low-cost thermal spray process are obtained through a parameter optimization.

**KEYWORDS:** Coatings; Flame chemistry; Nozzle diameter; Porosity; Stand-off distance

**Citation/Citar como:** Ruiz-Luna, H.; Méndez-Medrano, K.O.; Montoya Dávila, M.; Baltazar-Hernández, V.H. (2020). "Characterization of flame sprayed NiCrBSiMo coatings deposited with different spraying parameters". *Rev. Metal.* 56(2): e169. <https://doi.org/10.3989/revmetalm.169>

**RESUMEN:** *Caracterización de recubrimientos NiCrBSiMo depositados por rociado térmico por flama usando diferentes parámetros de depósito.* El presente trabajo reporta la optimización de los parámetros de procesamiento de un recubrimiento base Ni. El efecto de tres variables de depósito, *i.e.*, distancia de rociado, química de la flama y diámetro de la boquilla, fue evaluado sobre la estructura cristalina, porcentaje de porosidad, dureza y espesor del recubrimiento. El análisis se realizó en dos etapas, la primera consistió en determinar la influencia de la distancia de rociado sobre las características estructurales y microestructurales de los recubrimientos. En la segunda etapa se empleó un diseño de experimentos factorial 2<sup>2</sup> para evaluar el efecto del diámetro de la boquilla y la química de la flama sobre la porosidad, dureza y espesor del recubrimiento. Los resultados indicaron que la distancia de rociado afecta fuertemente la porosidad. A una distancia intermedia las partículas impactadas alcanzan un aplanamiento adecuado disminuyendo la porosidad, mientras que ésta última aumenta a distancias cortas y largas como resultado de la extensa o limitada deformación de las partículas al momento del impacto, respectivamente. De acuerdo a los resultados obtenidos del análisis del diámetro de la boquilla y la química de la flama, se observó que el primero tiene un efecto predominante en la microestructura y dureza de los recubrimientos. El uso de un diámetro pequeño de boquilla y una flama neutra reduce la porosidad e incrementa la dureza de los recubrimientos. Mediante la optimización de los parámetros se lograron obtener recubrimientos NiCrBSiMo con bajo contenido de porosidad y alto grado de dureza usando un proceso de rociado térmico de bajo costo.

**PALABRAS CLAVE:** Diámetro de boquilla; Distancia de rociado; Porosidad; Química de la flama; Recubrimientos

**ORCID ID:** Haideé Ruiz-Luna (<https://orcid.org/0000-0002-2799-8486>); Karla O. Méndez-Medrano (<https://orcid.org/0000-0001-6687-9239>); Miguel Montoya Dávila (<https://orcid.org/0000-0002-0443-029X>); Víctor H. Baltazar-Hernández (<https://orcid.org/0000-0001-8629-9936>)

**Copyright:** © 2020 CSIC. This is an open-access article distributed under the terms of the Creative Commons Attribution 4.0 International (CC BY 4.0) License.

## 1. INTRODUCTION

Self-fluxing alloys are widely used in chemical, petrochemical and mining industries due to their brazing characteristics and corrosion and wear properties (Miguel *et al.*, 2003; Navas *et al.*, 2006; Zeng *et al.*, 2016). These alloys consist of a Ni or Co matrix with additions of Cr, C, B, Si, Mo, Fe, and others, to improve their mechanical properties and corrosion resistance. For instance, Cr increases the hardness, corrosion and oxidation resistance (Otsubo *et al.*, 2000; Miguel *et al.*, 2003), additions of B and Si decrease the melting temperature and improve the self-fluxing capabilities of the alloys and also supports the formation of hard phases such as borides resulting in high hardness and wear resistance (Grigorescu *et al.*, 1995; Otsubo *et al.*, 2000; Navas *et al.*, 2006). These Ni-based alloys are employed as surface protective coatings to improve material performance and to extend the lifetime of industrial components and parts. Thermal spray technologies are feasible alternatives to deposit high-quality self-fluxing coatings with extensive industrial applications (Miguel *et al.*, 2003; Matsubara *et al.*, 2007; Liyanage *et al.*, 2010; Aussavy *et al.*, 2014; Zeng *et al.*, 2016). Nevertheless, the optimal properties of thermally sprayed coatings greatly depend on the deposition method, processing parameters conditions, and powder characteristics (Navas *et al.*, 2006; Liyanage *et al.*, 2010).

Combustion flame spraying technique is commonly used to deposit a wide range of materials, including Ni-based self-fluxing alloys, due to its low-cost, practical aspects and few environmental issues (Rodríguez *et al.*, 2003; Navas *et al.*, 2006; González *et al.*, 2007a; Amokrane *et al.*, 2011; Culliton *et al.*, 2013; Karimi *et al.*, 2016). Despite the above mentioned advantages; low particle velocity in flame spraying affects the microstructure and behavior of the coatings (Planche *et al.*, 2005). However, the mechanical properties and microstructural defects in terms of porosity, oxide content, presence of unmolten particles and cracks of thermally spray coatings also depend on the proper selection of spraying parameters (Mrdak *et al.*, 2009; Valarezo *et al.*, 2010; Ruiz-Luna *et al.*, 2014). Inappropriate selection and control of the deposition conditions result in a large amount of defects and therefore poor properties which reduces the performance of the coatings. In order to overcome such shortcomings and improve coatings quality; it is important to optimize the spraying parameters and to establish a correlation between the deposition variables and the resultant coatings characteristics. To date, previous investigations reported the microstructure and properties of flame sprayed coatings under a set of working conditions (González *et al.*, 2007b; Culliton *et al.*, 2013; Karimi *et al.*, 2016) without further analysis about

the optimization and correlation between the spraying parameters and coatings properties. Therefore, the aim of the present investigation is to analyze the effect of three process variables namely: stand-off distance, flame chemistry, and nozzle diameter, on the porosity content, hardness, and thickness of as-sprayed coatings, and to determine the processing conditions that allow the deposition of coatings with minimal microstructural defects using a more economical technique. The analysis is presented in two steps: in the first stage, the effect of the stand-off distance on the crystal structure and microstructure of the coatings is determined. In the second step, a simple 2<sup>2</sup> factorial design is employed and the effect of both: nozzle diameter and flame chemistry, on the crystal structure, porosity content, hardness and thickness of the coatings is presented and discussed.

## 2. MATERIALS AND METHODS

### 2.1. Coating deposition

Commercially available Ni-17.3Cr-4.5B-3.5Si-4.6Mo-2.9Fe-2.1Cu-1.2C (wt. %) powder was employed as feedstock material. The characteristics of the powder particles are shown in Fig. 1. The powder consists of mostly spherical particles although some irregular-shaped particles and particles with so-called satellites are observed in the micrograph (Fig. 1a). Distribution particle size ranges between 36 to 133  $\mu\text{m}$  with a mean particle size of 84  $\mu\text{m}$  (Fig. 1b) as measured by laser diffractometer (Helos/BR Sympatec). The SEM-EDS analysis of the cross section of the powder particle (inset of Fig. 1a), indicates that the microstructure consists of an enriched Ni matrix (bright gray phase) and a dark phase, mainly composed of Cr-rich particles, distributed in the Ni matrix.

The coatings were deposited using an oxyacetylene flame spray gun (CastoDyn DS 8000, Castolin Eutectic) onto grit-blasted low carbon steels plates of 50×25×4 mm. As mentioned, two stages were carried out in order to study the effect of the spraying parameters, (stand-off distance, flame chemistry, and nozzle diameter) on the coatings characteristics, including crystal structure, porosity percentage, hardness and thickness. On the first stage, the influence of the stand-off distance on the crystal structure and microstructure of the coatings was evaluated. Four stand-off distances were selected: 100, 150, 200, and 250 mm. At this stage, the coatings were deposited using neutral flame and the nozzle with diameter of 2.4 mm. On the second stage (Table 1), a simple 2<sup>2</sup> factorial design was set up to investigate the effect of the flame chemistry (two flame combinations, i.e. carburizing and neutral) and nozzle diameter using the porosity content, hardness and thickness of the coatings

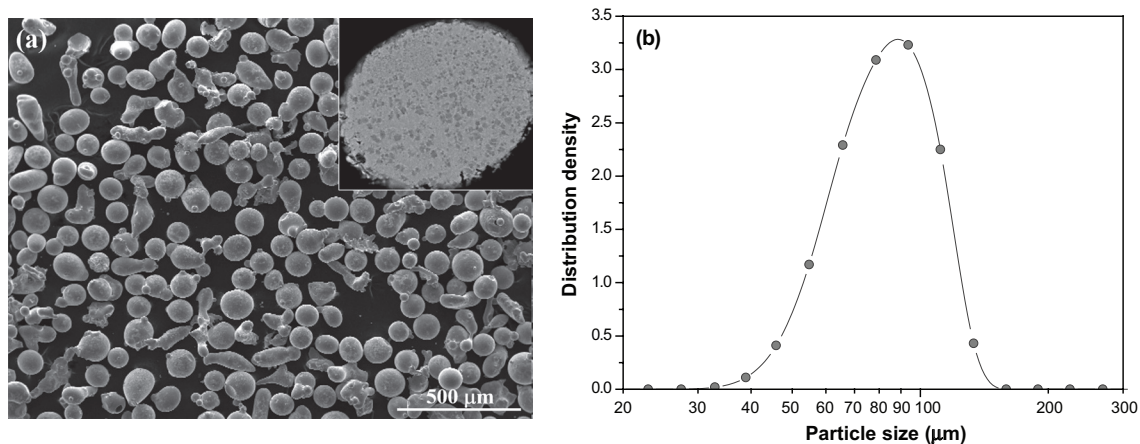


FIGURE 1. (a) Morphology and (b) particle size distribution of the NiCrBSiMo particles used as raw materials.

TABLE 1. Factorial design of experiments used on the second stage

Sample designation	Flame chemistry	Nozzle diameter (mm)
C1	Carburizing (-1)	2.4 (-1)
C2	Neutral (+1)	2.4 (-1)
C3	Carburizing (-1)	1.5 (+1)
C4	Neutral (+1)	1.5 (+1)

as response variables. The flame combinations were produced by changing the acetylene gas flow. The nozzles, designed specifically to the torch, are equal in length with a straight duct attached to the outlet of the converging section but its diameter is different (Table 1).

The oxygen and acetylene pressures were fixed to 4 and 0.7 Bar, respectively, in both stages. The number of torch passes over the substrate used in the first and second stages was one and three, respectively.

## 2.2. Characterization methods

X-ray diffraction (XRD, D8Advance Bruker diffractometer with Cu-K $\alpha$  radiation) technique was used to characterize the crystal structure of the coatings. A scanning electron (SEM, Philips XL30) microscope equipped with an energy-dispersive X-ray spectrometer (EDS) and an optical (Union Versamet 3) microscope were employed to analyze the cross-section and thickness of the samples. The porosity content of the coatings was determined by image analysis (ImageJ software) from 10 polished cross-section images. A Vickers indenter (Shimadzu) with a load of 300 g<sub>f</sub> and a dwell time of 15 s was used to measure the hardness of the coatings. An average of 10 indentations was carried out on each sample along their cross-section.

## 3. RESULTS

### 3.1. Effect of stand-off distance

Figure 2 shows the diffraction patterns of the feedstock powder and the as-sprayed coatings deposited at various stand-off distances. As observed, the coatings retained the original phases of the powder particles indicating that no phase transformation occurred during deposition. Ni is identified as the main phase, whereas phases corresponding to CrB, Ni<sub>3</sub>B, Ni-Si, and Cr<sub>3</sub>C<sub>2</sub> are also observed.

Based on microstructure observation in Fig. 3, as well as on the fraction of porosity in Fig 4; the coatings show up markedly differences related to the spraying distance. Samples deposited at short stand-off distances (100 and 150 mm, Fig. 3a and b, respectively) exhibited high porosity (Fig. 4) and significant unmolten and semi-molten particles, whereas a more homogeneous and dense microstructure with few unmolten particles are distinguished for the coating sprayed at a distance of 200 mm (Fig. 3c). However, by further increasing the stand-off distance the porosity increases up to ~15%. According to the above mentioned; it can be stated that coatings with low porosity content and a more homogeneous microstructure were obtained using medium stand-off distances. Therefore, for the second stage, the coatings were deposited using a spraying distance of 200 mm and the experiments were focused on the effect of the nozzle diameter and flame chemistry.

### 3.2. Influence of flame chemistry and nozzle diameter

The crystal structure of the coating sprayed employing the conditions shown in Table 1 are presented in Fig. 5. Similar to the X-ray results of the first stage, the analysis of the diffraction patterns

of the as-sprayed coatings revealed that Ni is still identified as the major phase and the corresponding intensities of CrB, Ni<sub>3</sub>B, Ni-Si, and Cr<sub>3</sub>C<sub>2</sub> are also detected. A broadening in the 41 to 50° range it is also noted for the C1 and C2 coatings.

According to the microstructural features of the coatings deposited upon the conditions listed in Table 1, there is a clear relationship between the nozzle diameter and the resultant microstructure of the coatings (Fig. 6). Coatings sprayed with a higher nozzle diameter, C1 and C2 (Fig. 6a and b), show the presence of unmolten particles and coating defects in terms of splat boundary separation and

voids resulting in high levels of porosity (~ 12%). In contrast, a lamellar structure with no visible unmolten or semi-molten particles and low coating porosity (2.7% in average) resulted for samples deposited with a lower nozzle diameter, C3 and C4 (Fig. 6c and d). The microstructure of the samples is quite similar irrespective of the flame chemistry; however, a slight reduction of porosity is observed when neutral flames are used, Fig. 6b and d, compared to the coatings deposited using a carburizing flame (Fig. 6a and c). A high magnification of the cross section of the flame sprayed coatings is presented in Fig. 7. The microstructure is quite similar

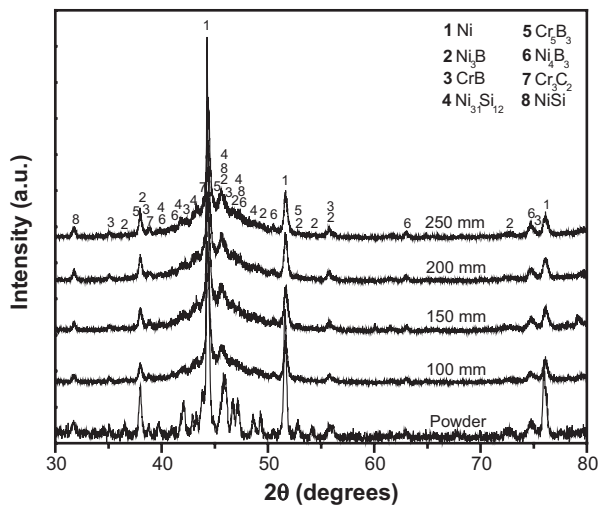


FIGURE 2. XRD patterns of the powder particles and coatings deposited at different stand-off distance.

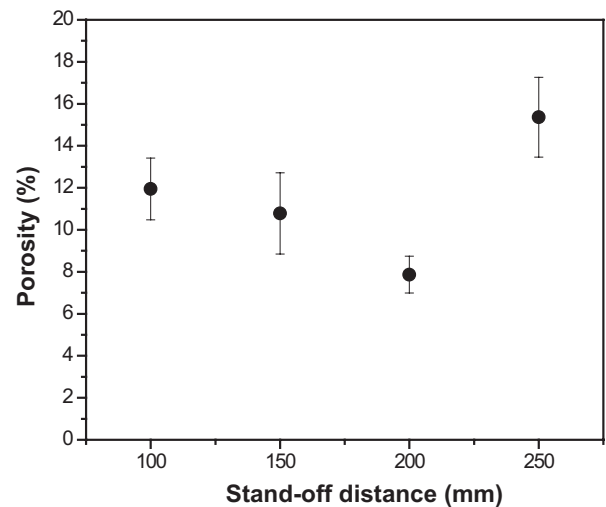


FIGURE 4. Porosity content of the as-sprayed coatings as a function of stand-off distance.

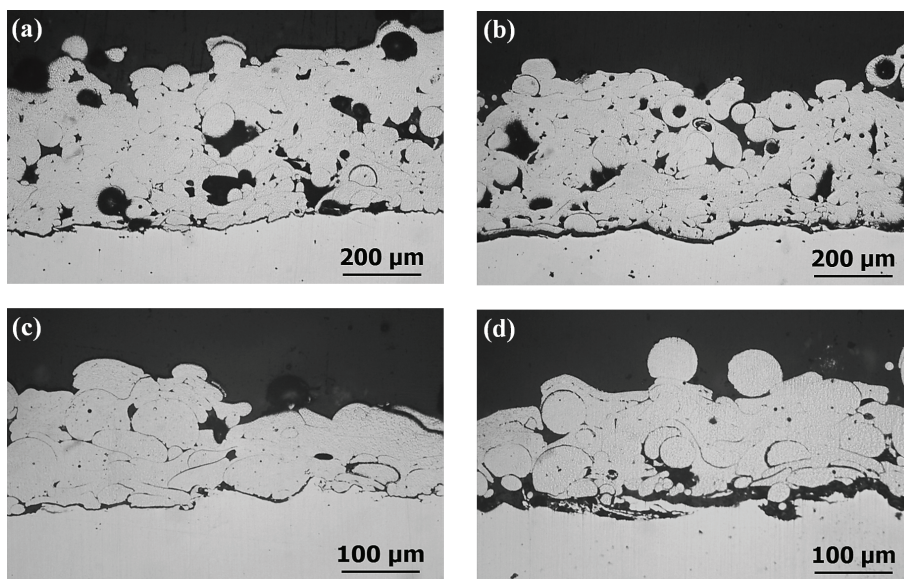


FIGURE 3. Microstructural characteristics of the coatings sprayed at different spraying distances: a) 100, b) 150, c) 200, and d) 250 mm.

to that of the powder particles (inset Fig. 1a). The coatings exhibit a homogeneous microstructure consisting of a bright matrix and fine precipitates uniformly distributed in the matrix (dark phase), irrespective of the spraying parameters. Compositional analysis revealed that the matrix is a Ni solid solution with Cr, Si, and Fe while the precipitates contain a high concentration of Cr with some additions of Si, Ni and Mo. Based on phase analysis previously reported for similar alloys, the matrix is identified as  $\gamma$ -Ni/Ni<sub>3</sub>B and the precipitates embedded in the matrix primarily correspond to CrB, Cr<sub>5</sub>B<sub>3</sub>, Ni<sub>3</sub>Si, Cr<sub>3</sub>C<sub>2</sub>, and Cr<sub>7</sub>C<sub>3</sub> (Kim *et al.*, 2003; Shrestha *et al.*, 2005; Linayage *et al.*, 2010; Hemmati *et al.*, 2013; Wen *et al.*, 2017). These results are consistent

with the X-ray analysis which showed the existence of these phases (Fig. 5).

The results of the factorial design of experiments are presented in Fig. 8. The main effect of each factor on the response variables i.e. porosity content, Vickers hardness, and thickness of the coatings is displayed in Fig. 8a-c, respectively. As published elsewhere (Montgomery, 1991), these values were computed by averaging the response variable performed with the high (or low) level of each variable, irrespective of the value of the other variable.

In accordance with Fig. 8, the nozzle diameter significantly influences the coatings characteristics. The use of small nozzle diameter results in low porosity meanwhile large diameters increase the levels of porosity around 12% (Fig. 8a). Regarding the hardness and thickness of the samples, these responses are also favored by small nozzle diameters as shown in Fig. 8b and c. Hence, coatings deposited with small nozzle diameters (C3 and C4) exhibited

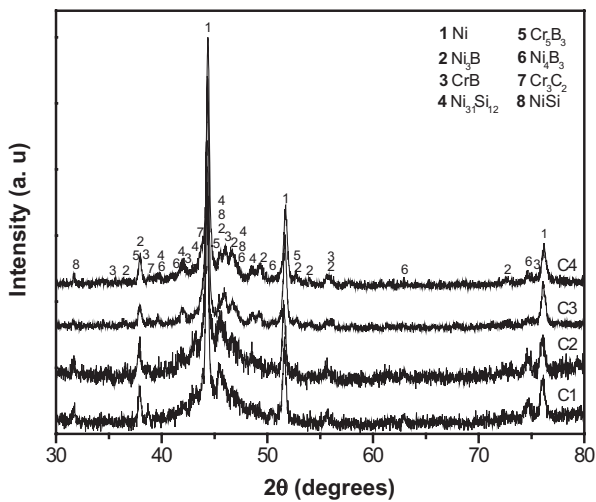


FIGURE 5. X-ray patterns of the as-sprayed coatings deposited using different nozzle diameter and flame chemistry (Table 1).

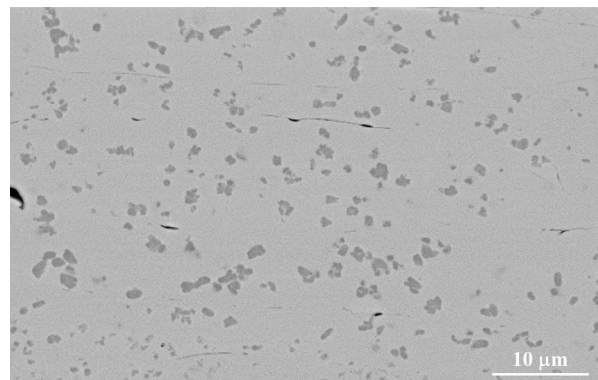


FIGURE 7. Micrograph showing the microstructure of the flame sprayed coatings.

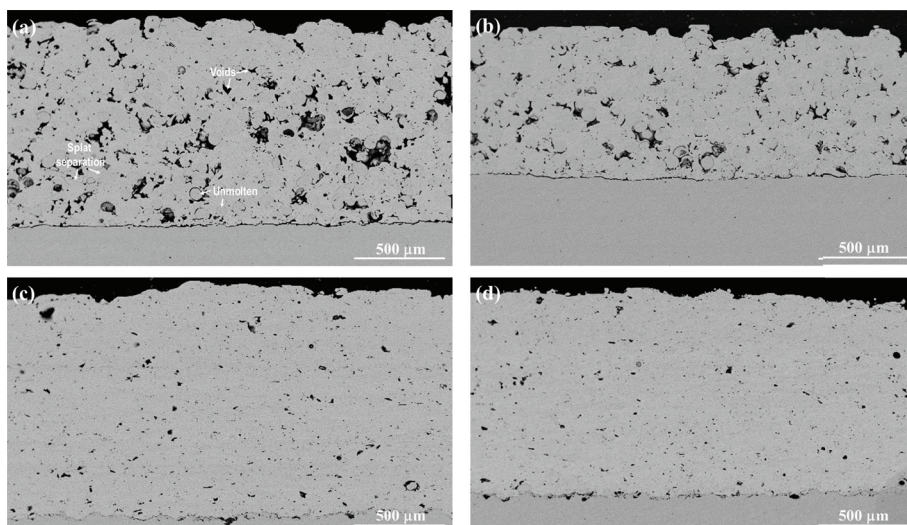


FIGURE 6. Cross-section of the coatings sprayed using distinct nozzle diameter and flame chemistry: a) C1, b) C2, c) C3, and d) C4.

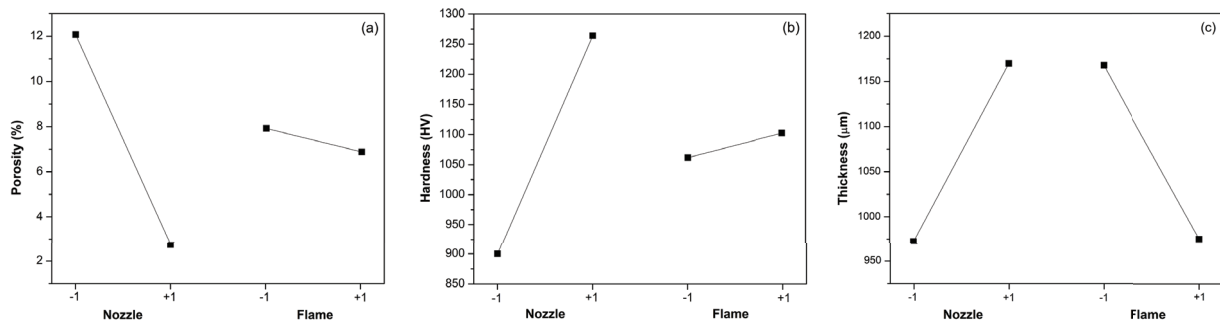


FIGURE 8. Influence of nozzle diameter and flame chemistry on a) porosity percentage, b) hardness, and c) thickness of the coatings.

higher hardness, thickness and reduced porosity as compared with samples sprayed with large diameters (C1 and C2).

It is important to notice that the flame chemistry barely affects the porosity and hardness, Fig. 8a–b, however an influence on the thickness of the coatings is observed (Figs. 6 and 8c). Thinner coatings with high hardness and low porosity percentage are obtained when using neutral flames.

#### 4. DISCUSSION

The microstructure of the coatings is significantly influenced by the stand-off distance as pointed out in previous section. It has been reported that the substrate temperature, residence time of the particles in the flame, and the in-flight particle characteristics, *i.e.* velocity and temperature, depend on the spraying distance (Mrdak *et al.*, 2009; Valarezo *et al.*, 2010; Ruiz-Luna *et al.*, 2014). For instance, at short spraying distances (for example 100 or 150 mm), particles impact the substrate at elevated temperature causing significant levels of splashing and therefore high porosity (Mrdak *et al.*, 2009; Dobler *et al.*, 2000; Valarezo *et al.*, 2010; Ruiz-Luna *et al.*, 2014). At intermediate distance, (200 mm) it seems that the powder particles attained an adequate velocity and temperature resulting in a balance between particle flattening and solidification which decreases the porosity content. At longer spraying distances ( $\geq 250$  mm), the porosity of the coatings and the unmolten particles increase due to the limited particle deformation at impact. Hence, the powder particles reached the substrate in a resolidified or cooled state because the residence time of the particles in the flame increases resulting in lower particle velocities (He *et al.*, 2001; Valarezo *et al.*, 2010; Ruiz-Luna *et al.*, 2014).

As observed in the XRD patterns in Fig. 5, coatings C1 and C2 showed a peak broadening between  $41$  to  $50^\circ$  which may be associated to a slight amorphization or slow crystallization of the self-fluxing powder particles due to the high cooling rates attained during solidification as reported previously

(Guo *et al.*, 1995; Gruzdyś *et al.*, 2009; Zeng *et al.*, 2009). For instance, Planche *et al.* (2005) have reported that the recrystallization of the NiCrBSi particles after impact is difficult because the presence of B and Si within the alloy.

According to the results of the second stage, the coating characteristics are also affected by the nozzle diameter. A variation in nozzle diameter seems to produce distinct energy of the gas which indeed is transmitted to the powder particles. Because in flame spray process the flame velocity ( $< 100 \text{ m}\cdot\text{s}^{-1}$ ) (Pawloski, 2008) is lower compared to the speed of sound; then it is to be assumed that the gas flow behaves as incompressible manner. In accordance to the principles of fluid dynamics, ducts with lower area exit increases the velocity of the flow and vice versa (Mott, 1996). Based on this, it is expected that the nozzle with lower diameter produces a higher kinetic energy of the particles than the nozzle with a large diameter and thus, distinct microstructural features due to the flattening degree of the particles is affected by the in-flight particle characteristics *i.e.*, velocity and temperature (Planche *et al.*, 2005). Therefore, particles upon C1 and C2 conditions have lower particle velocity than those of C3 and C4 conditions. Nozzle with large diameter (samples C1 and C2, associated with low velocities) are unable to spread and plastically deform the powder particles at impact. Thus, the microstructure of the coatings resulted with large unmolten and partially molten particles (Fig. 6a-b) that increases the porosity and decreases the hardness of the coatings, Fig. 8a-b, respectively. Thinner coatings probably result as a consequence of debonding of unmolten and cooled particles at impact. On the contrary, coatings C3 and C4 sprayed with lower diameter showed a lamellar structure with reduced porosity, these characteristics are attributed to a higher kinetic energy of the particles, compared with C1 and C2 conditions, which increases the splat cohesion and ensures a balance of plastic deformation and solidification at the impingement onto the substrate (Fig. 6c-d), and thereby low porosity and high hardness and thickness (Fig. 8).

The observation of the hardness reveals that this parameter is in direct correlation with the inherent microstructure of the coatings. As mentioned before, high kinetic energies improved the microstructure of the coatings by increasing the cohesion and density of the sprayed particles resulting in higher coating hardness. These conditions are achieved using small nozzle diameters and neutral flames (Fig. 8b).

It is worth nothing that the use of small nozzles contributes to reduce the porosity by about 4 times (from 12.1% to 2.7%) and increase the hardness from 900 to 1264 HV. Similar porosity (Miguel *et al.*, 2003; Shrestha *et al.*, 2005; Yu *et al.*, 2013; Singh and Kaur, 2016; Wen *et al.*, 2017) and hardness (González *et al.*, 2007a; González *et al.*, 2007b; Singh and Kaur, 2016) values have been reported for thermally sprayed Ni-based coatings. However, the porosity content obtained in the present study for C3 and C4 conditions (2.7% in average), is lower compared to those reported for as-sprayed self-fluxing coatings deposited by flame and plasma spraying (Higuera Hidalgo *et al.*, 2001; Kim *et al.*, 2003; Planche *et al.*, 2005; Culliton *et al.*, 2013; Bergant *et al.*, 2014).

Concerning the flame chemistry, this parameter influences the temperature of combustion spray systems (Pawloswski, 2008); the maximum flame temperatures are reached near the stoichiometric or neutral condition as stated previously (Valarezo *et al.*, 2010; Ruiz-Luna *et al.*, 2014; Jadidi *et al.*, 2015). This statement is in accordance with the microstructural results in this study where higher particle heating results in superior degree of particle flattening and bonding at impact and subsequent high hardness and low porosity and thickness (Fig. 8a-c).

In summary, the microstructure, pore content and hardness of the coatings are dependent on the deposition parameters; namely, spraying distance and nozzle diameter, and an optimum selection of these leads to an improvement of coatings properties. Proper deformation and spreading of the particles is attained when medium stand-off distances, small nozzles diameter and neutral flames are employed.

## 5. CONCLUSIONS

- The porosity of the coatings shows a direct correlation with the stand-off distance, intermediate distance leads to formation of dense and homogeneous flame spray coatings with acceptable properties.
- The nozzle diameter has a predominant influence on the splat morphology and coatings properties. By employing small diameters, coatings exhibited a lamellae structure with low porosity and high hardness compared with those deposited using large diameters indicating good

consolidation. A significant reduction in porosity is obtained after parameters optimization.

- The hardness depends primarily on the morphological features of the coating, which is improved by employing neutral flames and small nozzle diameters.
- Good-quality Ni-based coatings using a low-cost thermal spray process are obtained through a parameter optimization, low porosity and high hardness flame spray coatings are obtained when using a small nozzle diameter, neutral flame, and an intermediate distance.

## ACKNOWLEDGMENTS

Authors are gratefully acknowledged to Consejo Nacional de Ciencia y Tecnología (CONACyT - México) for financial support under projects No. 270613-INFRA-2016 and 254731-INFRA-2015. Authors also thank the program Cátedras-Conacyt and Aixa Ibeth Gutiérrez Pérez and Alma Gabriela Mora García for the laser diffractometer and electron microscopy measurements carried out at CENAPROT and LIDTRA National Laboratories, respectively.

## REFERENCES

- Amokrane, B.M., Abdelhamid, S., Youcef, M., Abderrahim, G., Nedjemeddine, B., Ahmed M. (2011). Microstructural and Mechanical Properties of Ni-Base Thermal Spray Coatings Deposited by Flame Spraying. *Mater. Trans. B* 42, 932–938. <https://doi.org/10.1007/s11663-011-9551-0>.
- Aussavy, D., Costil, S., El Kedim, O., Montavon, G., Bonnot, A.F. (2014). Metal Matrix Composite Coatings Manufactured by Thermal Spraying: Influence of the Powder Preparation on the Coating Properties. *J. Therm. Spray Tech.* 23 (1–2), 190–196. <https://doi.org/10.1007/s11666-013-9999-3>.
- Bergant, Z., Trdan, U., Grum, J. (2014). Effect of high-temperature furnace treatment on the microstructure and corrosion behavior of NiCrBSi flame-sprayed coatings. *Corros. Sci.* 88, 372–386. <https://doi.org/10.1016/j.corsci.2014.07.057>.
- Culliton, D., Betts, A., Carvalho, S., Kennedy, D. (2013). Improving Tribological Properties of Cast Al-Si Alloys through Application of Wear-Resistant Thermal Spray Coatings. *J. Therm. Spray Tech.* 22 (4), 491–501. <https://doi.org/10.1007/s11666-013-9894-y>.
- Dobler, K., Kreye, H., Schwetzke, R. (2000). Oxidation of stainless steel in the high velocity oxy-fuel process. *J. Therm. Spray Tech.* 9, 407–413. <https://doi.org/10.1361/105996300770349872>.
- González, R., García, M.A., Peñuelas, I., Cadenas, M., Fernández, R., Hernández Battez, A., Felgueroso, D. (2007a). Microstructural study of NiCrBSi coatings obtained by different processes. *Wear* 263 (1-6), 619–624. <https://doi.org/10.1016/j.wear.2007.01.094>.
- González, R., Cadenas, M., Fernández, R., Cortizo, J.L., Rodríguez, E. (2007b). Wear Behaviour of Flame Sprayed NiCrBSi Coating Remelted by Flame or by Laser. *Wear* 262 (3-4), 301–307. <https://doi.org/10.1016/j.wear.2006.05.009>.
- Grigorescu, I.C., Di Rauso, C., Drira-Halouani, R., Lavelle, B., Di Giampaolo, R., Lira, J. (1995). Phase characterization in Ni alloy-hard carbide composites for fused coatings. *Surf. Coat. Tech.* 76–77, 494–498. [https://doi.org/10.1016/0257-8972\(95\)02511-1](https://doi.org/10.1016/0257-8972(95)02511-1).
- Gruzdis, E., Meškiniš, S., Juraitis, A. (2009). Influence of WC/Co Concentration on Structure and Mechanical Properties

- of the Thermally Sprayed WC/Co-NiCrBSi Coatings. *Materials Science* 15 (1), 35–39.
- Guo, D.Z., Li, F.L., Wang, J.Y., Sun, J.S. (1995). Effects of post-coating processing on structure and erosive wear characteristics of flame and plasma spray coatings. *Surf. Coat. Tech.* 73 (1–2), 73–76. [https://doi.org/10.1016/0257-8972\(94\)02364-6](https://doi.org/10.1016/0257-8972(94)02364-6).
- He, J., Ice, M., Lavernia, E. (2001). Particle Melting Behavior during High-Velocity Oxygen Fuel Thermal Spraying. *J. Therm. Spray Tech.* 10 (1), 83–93. <https://doi.org/10.1361/105996301770349547>.
- Hemmati, I., Rao, J.C., Ocelik, V., De Hosson, J.Th.M. (2013). Electron Microscopy Characterization of Ni-Cr-B-Si-C Laser Deposited Coatings. *Microsc. Microanal.* 19 (1), 120–131. <https://doi.org/10.1017/S1431927612013839>.
- Higuera Hidalgo, V., Belzunce Varela, F.J., Carriles Menéndez, A., Poveda Martínez, S. (2001). A Comparative Study of High-Temperature Erosion Wear of Plasma-Sprayed NiCrBSiFe and WC-NiCrBSiFe Coatings under Simulated Coal-Fired Boiler Conditions. *Tribol. Int.* 34 (3), 161–169. [https://doi.org/10.1016/S0301-679X\(00\)00146-8](https://doi.org/10.1016/S0301-679X(00)00146-8).
- Jadidi, M., Moghtadernejad, S., Dolatabadi, A. (2015). A Comprehensive Review on Fluid Dynamics and Transport of Suspension/Liquid Droplets and Particles in High-Velocity Oxygen-Fuel (HVOF) Thermal Spray. *Coatings* 5 (4), 576–645. <https://doi.org/10.3390/coatings5040576>.
- Karimi, M.R., Salimijazi, H.R., Golozar, M.A. (2016). Effects of Remelting Processes on Porosity of NiCrBSi Flame Sprayed Coatings. *Surf. Eng.* 32 (3), 238–243. <https://doi.org/10.1179/1743294415Y.0000000107>.
- Kim, H.-J., Hwang, S.-Y., Lee, C.-H., Juvanon, P. (2003). Assessment of wear performance of flame sprayed and fused Ni-based coatings. *Surf. Coat. Tech.* 172 (2-3), 262–269. [https://doi.org/10.1016/S0257-8972\(03\)00348-7](https://doi.org/10.1016/S0257-8972(03)00348-7).
- Liyanage, T., Fisher, G., Gerlich, A.P. (2010). Influence of alloy chemistry on microstructure and properties in NiCrBSi overlay coatings deposited by plasma transferred arc welding (PTAW). *Surf. Coat. Tech.* 205 (3), 759–765. <https://doi.org/10.1016/j.surfcoat.2010.07.095>.
- Matsubara, Y., Sochi, Y., Tanabe, M., Takeya, A. (2007). Advanced Coatings on Furnace Wall Tubes. *J. Therm. Spray Tech.* 16 (2), 195–201. <https://doi.org/10.1007/s11666-007-9030-y>.
- Miguel, J.M., Guilemany, J.M., Vizcaino, S. (2003). Tribological Study of NiCrBSi Coating Obtained by Different Processes. *Tribol. Int.* 36 (3), 181–187. [https://doi.org/10.1016/S0301-679X\(02\)00144-5](https://doi.org/10.1016/S0301-679X(02)00144-5).
- Montgomery, D.C. (1991). *Diseño y Análisis de Experimentos*. Grupo Editorial Iberoamérica, México.
- Mott, R. (1996). *Applied Fluid Mechanics*. Prentice-Hall Hispanoamericana, Englewood Cliffs.
- Mrdak, M., Vencl, A., Cosic, M. (2009). Microstructure and Mechanical Properties of the Mo-NiCrBSi Coating Deposited by Atmospheric Plasma Spraying. *FME Transactions* 37, 27–32.
- Navas, C., Colaço, R., De Damborenea, J., Vilar, R. (2006). Abrasive wear behaviour of laser clad and flame sprayed-melted NiCrBSi coatings. *Surf. Coat. Tech.* 200 (24), 6854–6862. <https://doi.org/10.1016/j.surfcoat.2005.10.032>.
- Otsubo, F., Era, H., Kishitake, K. (2000). Structure and Phases in Nickel-Base Self-Fluxing Alloy Coating Containing High Chromium and Boron. *J. Therm. Spray Tech.* 9 (1), 107–113. <https://doi.org/10.1361/105996300770350131>.
- Pawlowski, L. (2008). *The Science and Engineering of Thermal Spray Coatings*. John Wiley & Sons, Ltd, England.
- Planche, M.P., Liao, H., Normand, B., Coddet, C. (2005). Relationships between NiCrBSi Particle Characteristics and Corresponding Coating Properties Using Different Thermal Spraying Processes. *Surf. Coat. Tech.* 200 (7), 2465–2473. <https://doi.org/10.1016/j.surfcoat.2004.08.224>.
- Rodríguez, J., Martín, A., Fernández, R., Fernández, J.E. (2003). An experimental study of the wear performance of NiCrBSi thermal spray coatings. *Wear* 255 (7-12), 950–955. [https://doi.org/10.1016/S0043-1648\(03\)00162-5](https://doi.org/10.1016/S0043-1648(03)00162-5).
- Ruiz-Luna, H., Lozano-Mandujano, D., Alvarado-Orozco, J.M., Valarezo, A., Poblano-Salas, C.A., Trápaga-Martínez, L.G., Espinoza-Beltrán, F.J., Muñoz-Saldaña, J. (2014). Effect of HVOF Processing Parameters on the Properties of NiCoCrAlY Coatings by Design of Experiments. *J. Therm. Spray Tech.* 23 (6), 950–961. <https://doi.org/10.1007/s11666-014-0121-2>.
- Shrestha, S., Hodgkiess, T., Neville, A. (2005). Erosion-corrosion behaviour of high-velocity oxy-fuel Ni-Cr-Mo-Si-B coatings under high-velocity seawater jet impingement. *Wear* 259 (1–6), 208–218. <https://doi.org/10.1016/j.wear.2005.01.038>.
- Singh, S., Kaur, M. (2016). Mechanical and Microstructural Properties of NiCrFeSiBCr/Cr<sub>2</sub>C<sub>3</sub> Composite Coatings – Part I. *Surf. Eng.* 32 (7), 464–474. <https://doi.org/10.1179/1743294414Y.0000000416>.
- Valarezo, A., Choi, W.B., Chi, W., Gouldstone, A., Sampath, S. (2010). Process Control and Characterization of NiCr Coatings by HVOF-DJ2700 System: A Process Map Approach. *J. Therm. Spray Tech.* 19 (5), 852–865. <https://doi.org/10.1007/s11666-010-9492-1>.
- Wen, Z.H., Bai, Y., Yang, J.F., Huang, J. (2017). Corrosion resistance of vacuum re-melted Ni60-NiCrMoY alloy coatings. *J. Alloys Compd.* 711, 659–669. <https://doi.org/10.1016/j.jallcom.2017.03.318>.
- Yu, H., Zhang, W., Wang, H., Guo, Y., Wei, M., Song, Z., Wang, Y. (2013). Bonding and sliding wear behaviors of the plasma sprayed NiCrBSi coatings. *Tribol. Int.* 66, 105–113. <https://doi.org/10.1016/j.triboint.2013.04.017>.
- Zeng, Z., Kuroda, S., Era, H. (2009). Comparison of oxidation behavior of Ni–20Cr alloy and Ni-base self-fluxing alloy during air plasma spraying. *Surf. Coat. Tech.* 204 (1-2), 69–77. <https://doi.org/10.1016/j.surfcoat.2009.06.036>.
- Zeng, Q., Sun, J., Emori, W., Jiang, S.L. (2016). Corrosion Behavior of Thermally Sprayed NiCrBSi Coating on 16MnR Low-Alloy Steel in KOH Solution. *J. Mater. Eng. Perform.* 25 (5), 1773–1780. <https://doi.org/10.1007/s11665-016-2012-9>.